



HAL
open science

Ferroceneboronic Acid and Derivatives Synthesis, Structure, Electronic Properties, and Reactivity in Directed C-H Bond Activation

W. Erb, J.-P. Hurvois, T. Roisnel, V. Dorcet

► **To cite this version:**

W. Erb, J.-P. Hurvois, T. Roisnel, V. Dorcet. Ferroceneboronic Acid and Derivatives Synthesis, Structure, Electronic Properties, and Reactivity in Directed C-H Bond Activation. *Organometallics*, 2018, 37 (21), pp.3780-3790. 10.1021/acs.organomet.8b00501 . hal-01939028

HAL Id: hal-01939028

<https://univ-rennes.hal.science/hal-01939028>

Submitted on 14 Dec 2018

HAL is a multi-disciplinary open access archive for the deposit and dissemination of scientific research documents, whether they are published or not. The documents may come from teaching and research institutions in France or abroad, or from public or private research centers.

L'archive ouverte pluridisciplinaire **HAL**, est destinée au dépôt et à la diffusion de documents scientifiques de niveau recherche, publiés ou non, émanant des établissements d'enseignement et de recherche français ou étrangers, des laboratoires publics ou privés.

Ferroceneboronic acid and derivatives: synthesis, structure, electronic properties and reactivity in directed C-H bond activation.

William ERB^{*,†}, Jean-Pierre HURVOIS,[†] Thierry ROISNEL[†] and Vincent DORCET[†]

[†] Univ Rennes, CNRS, ISCR (Institut des Sciences Chimiques de Rennes) – UMR 6226, F-35000 Rennes, France.

Supporting Information

ABSTRACT: Known since 1959, ferroceneboronic acid (**1**) and its derivatives have been mainly used as polyol sensors and in cross-coupling reactions. However, a literature survey revealed that there is not a paper describing the full characterization of ferroceneboronic acid derivatives and that useful boron protecting groups have not been studied in the ferrocene series. Here, we present an optimized multigram scale synthesis of the known ferroceneboronic acid (**1**) using a phase-switch purification process. It was furthermore functionalized to reach the diamionaphthalene (FcB(dan), **15**), anthranilamides (FcB(aam), **16**; FcB(Me-aam), **17** and **18**), potassium trifluoroborate (FcBF₃K, **19**), triolborate (FcB(triolborate), **20**) and *N*-methyliminodiacetic acid (FcB(MIDA), **21**) derivatives. Their structures were unambiguously assigned by NMR and X-ray analysis and the data collected provided a general overview of the electronic and structural features of these compounds. From the data obtained, B(dan) and B(aam) groups were classified as electron-withdrawing whereas trifluoroborate and triolborate behave as electron-donating groups. We report the first catalytic silylation of ferrocene C-H bonds to access di- and trisubstituted derivatives. Catalytic borylation was also attempted, highlighting a switch of regioselectivity that was unambiguously assigned by X-ray analysis.

INTRODUCTION

The discovery of ferrocene 65 years ago rejuvenated the area of organometallic chemistry and the 1973 Nobel Prize for Chemistry was therefore awarded to Fischer and Wilkinson for their work. This organometallic scaffold fastly imposed itself as one of the most used sensor due to its reversible redox properties and has found numerous applications as ligand in organometallic chemistry.¹ Recent years have witnessed the emergence of ferrocene-based material chemistry and various applications of this organometallic compound in medicinal chemistry.² Unsubstituted ferrocenium salts can be obtained from ferrocene by oxidation and their use in synthesis was recently reviewed.³ Similarly, substituted ferrocenium salts can also behave as one-electron oxidant or Lewis acids as exemplified by the work of Jahn and Hall, respectively.⁴

In the course of carbon-heteroatom bond formation studies in the ferrocene series,⁵ we became interested in the synthesis and use of ferroceneboronic acid and its derivatives (Figure 1). However, a literature survey revealed striking differences in the analytical descriptions of such compounds.

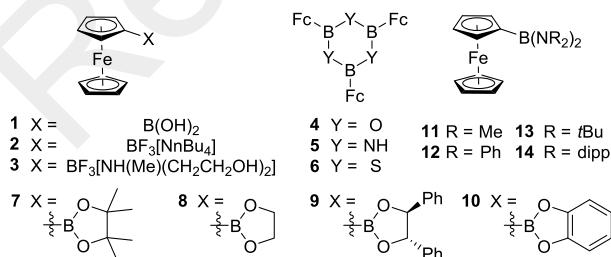


Figure 1. Ferroceneboronic acid (**1**) and selected derivatives **2-14**. Fc = ferrocenyl, dipp = 2,6-diisopropylphenyl.

The case of ferroceneboronic acid (FcB(OH)₂, **1**) is highly relevant: initially prepared by Nesmejanov in 1959 from ferrocenyllithium and tributylborate, it was characterized by its melting point and elemental analysis.⁶ Later prepared by Helling⁷ (1961) and Pauson⁸ (1967), it is only in 1970 that Post described its mass spectrometry analysis.⁹ Interestingly, he noticed the tendency of FcB(OH)₂ to dehydration, leading to variable amounts of the corresponding boroxine (**4**), which complicates its analysis. In 1978, Illuminati measured the pK_a of FcB(OH)₂ and reported its ¹H NMR spectra in deuterated acetone.¹⁰ However, only the ¹H signal of the boronic acid group was attributed by deuterium exchange. Christensen later described a similar ¹H NMR spectrum in deuterated chloroform.¹¹ However, to the best of our knowledge, the only copy of ¹H NMR spectrum available could be found in the work of Lacina who followed FcB(OH)₂ titration with diols by NMR.¹² In 2004 Aldridge reported the X-ray diffraction analysis of **1** and the hydrogen bonding network developed at the solid state.¹³ Finally, Voloshin reported the UV-spectrum of FcB(OH)₂ in 2008.¹⁴

The case of the trifluoroborate salts, relevant ferroceneboronic acid derivatives,¹⁵ is also interesting. Tetra-*n*-butylammonium ferrocenyltrifluoroborate (**2**) was initially prepared by Lough in 2001.¹⁶ The identity of the compound was clearly established by X-ray diffraction analysis and no other analyses were performed. Two years later, Bats reported the synthesis and crystal structure of ferricenyltrifluoroborate.¹⁷ Although the C-B bond length was little affected upon oxidation of Fe²⁺ to Fe³⁺, he noticed a slight elongation (0.04 Å) of the Fe-C bond. In 2005, Aldridge reported for the first time the full characterization of ferrocenyltrifluoroborate with an ammonium counter anion (**3**).¹⁸ Although unattributed ¹H, ¹³C, ¹¹B and ¹⁹F NMR spectra were described. The structure of the product was further supported by IR spectroscopy, mass spectrometry

and X-ray diffraction analysis. Finally, Grzybowski reported in 2014 the formation of ferrocenyltrifluoroborate, and its characterization by IR spectroscopy, elemental analysis and electrochemical measurements.¹⁹

On the other hand, triferrocenylboroxine (**4**) and the related triferrocenylborazine (**5**) and triferrocenyltrithiaborine (**6**) have been more studied. Originally reported by Post in 1970,⁹ various analytical data can be found in the literature (¹H, ¹³C, ¹¹B, ⁵⁷Fe NMR data, IR and mass spectra, elemental analysis)²⁰ and it should be noted that, in the solid state, the three ferrocenyl groups are generally arranged on the same side of the central six-membered ring.²¹

Boronic esters and diaminoboryl derivatives are also well represented in the literature, the former notably due to the ability of ferroceneboronic acid to react with diols and sugars.^{12, 22} Various 5-membered boronic esters such as pinacol (**7**), ethyleneglycol (**8**), hydrobenzoin (**9**) or catechol (**10**) derivatives have also been prepared and characterized.²³ Finally, full analytical data could be found for the various diaminoborylferrocenes **11-14**.²⁴

Therefore, it appears that ferroceneboronic acid (**1**) and potassium trifluoroborate (**19**) remain to be fully characterized. Furthermore, to the best of our knowledge, recently developed boron-protecting groups such as 1,8-diaminonaphthalene (dan),²⁵ anthranilamide (aam),²⁶ cyclic triolborates²⁷ and *N*-methyliminodiacetic acid (MIDA)²⁸ have never been introduced onto FcB(OH)₂, although their utility in cross-coupling reactions has been fully demonstrated.²⁹ Finally, owing to the growing importance of azaborine chemistry,³⁰ it would be of high interest to be able to access the ferrocenic analog of known compounds to elucidate their specific properties.

Here, we report our study of the known FcB(OH)₂ (**1**, Figure 2) and its original diaminonaphthalene (FcB(dan), **15**), boron-anthranilamides (FcB(aam), **16**; FcB(Me-aam), **17** and **18**), potassium trifluoroborate (FcBF₃K, **19**), triolborate (FcB(triolborate), **20**) and *N*-methyliminodiacetic acid (FcB(MIDA), **21**) derivatives. NMR, X-ray diffraction and electrochemical analysis were performed to classify these borylated groups in terms of electron-donating and -withdrawing capacity. Finally, ferrocene catalytic silylation and borylation by C-H activation, directed by the boron anthranilamide group, is described.

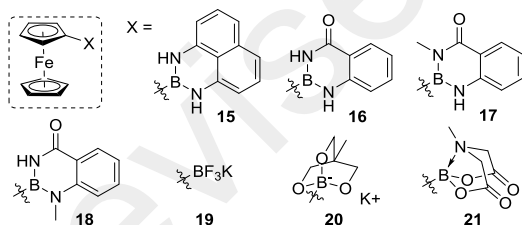
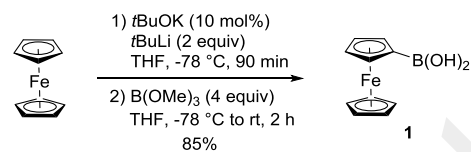


Figure 2. Ferroceneboronic acid derivatives prepared and characterized in this study.

Results and discussion

Synthesis of ferroceneboronic acid and its derivatives. Historically, ferroceneboronic acid (**1**) was prepared by deprotonation of ferrocene using butyllithium before interception of the resulting lithioferrocene with tributylborate.^{6b, 7} However, mixtures of ferroceneboronic acid (**1**) and 1,1'-ferrocenylenediboronic acid were invariably obtained. Pauson later described the reaction of ferrocenyl dihaloborane with water to generate FcB(OH)₂ in yields up to 55%.⁸ Here, we report a modification

of the Nesmeyanov procedure based on the use of *t*BuLi in presence of catalytic *t*BuOK.³¹ Employing the phase-switch purification developed by Hall,³² ferroceneboronic acid (**1**) was obtained on a multigram scale in 85% yield, pure enough for most applications without the requirement of chromatographic purification (Scheme 1).



Scheme 1. Synthesis of ferroceneboronic acid (**1**).

Boron naphthalene-1,8-diamido derivatives are obtained by the reaction of boronic acids with 1,8-diaminonaphthalene under azeotropic removal of water. In our hands, the procedure developed by Sugimoto²⁵ afforded FcB(dan) (**15**) in a surprisingly low yield (Table 1, entry 1). Concerned by the potential presence of anhydrides, a hydrolysis step was added, but with minor success (entry 2). Although still moderate, best results were finally obtained using the FeCl₃/imidazole catalytic system developed by Pucheault (entry 3).³³

Table 1. Formation of FcB(dan) (**15**).

Entry	Conditions	Yield (%)
1	Toluene, reflux, 16 h	27
2	i) Toluene, water, rt, 15 min; ii) Reflux, 16 h	31
3	FeCl ₃ (5 mol%), imidazole (3 equiv), MeCN, H ₂ O, rt, 16 h	44

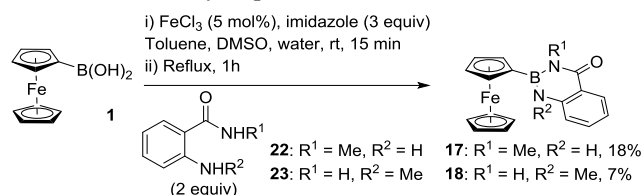
Likewise, the formation of the boron-anthranilamide group relies on the esterification of the boronic acid with anthranilamide. Following the procedure described by Sugimoto,²⁶ FcB(aam) (**16**) was isolated in a moderate yield after column chromatography (Table 2, entry 1). Better results were noticed when adding an initial hydrolysis step (entry 2), whereas the FeCl₃/imidazole catalytic system always afforded **16** in moderate yields, probably due to the lower nucleophilicity of anthranilamide when compared to 1,8-diaminonaphthalene (entries 3 and 4).

Table 2. Formation of FcB(aam) (**16**).

Entry	Conditions	Yield (%)
1	Toluene, reflux, 16 h	58
2	i) Toluene, water, rt, 15 min; ii) Reflux, 16 h	71
3	FeCl ₃ (5 mol%), imidazole (3 equiv), MeCN, H ₂ O, rt, 6 h	33
4	FeCl ₃ (5 mol%), imidazole (3 equiv), MeCN, H ₂ O, rt, 120 h	61

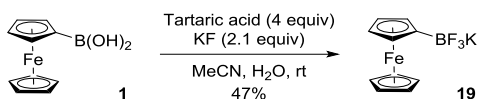
The formation of the methylated anthranilamide derivatives **17** and **18** was more difficult. Indeed, heating at toluene reflux **1** with either **22** or **23** only afforded traces of products, whereas the FeCl₃/imidazole system was unable to catalyze the reaction, even with prolonged reaction time (Scheme 2). It was finally found that complete conversion could be reached by heating at toluene reflux **1** and **22** or **23** in the presence of FeCl₃ and im-

idazole under azeotropic removal of water. However, the instability of **17** and **18** led to major degradation during the purifications. As the introduction of the methyl groups does not significantly affect the structures of the anthranilamides, as judged by NMR and X-ray diffraction analysis, the origin of this instability remains unclear. Hydrolysis, protodeboronation or oxidation appears as possible decomposition pathways, although none of them could currently be preferred.



Scheme 2. Formation of FcB(Me-aam) (**17** and **18**).

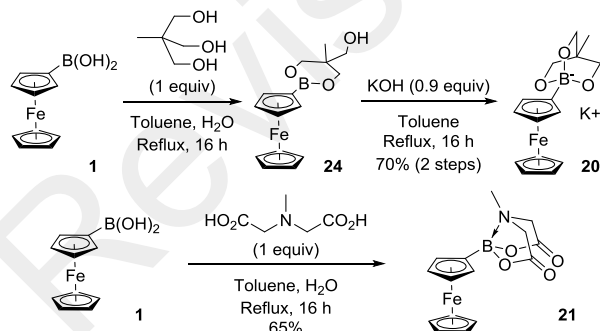
Potassium trifluoroborate salts are usually prepared by reacting boronic acids with KHF₂ according to Vedejs.³⁴ Even if the generality of this method remains incontestable, corrosive KHF₂ causes etching of glassware and Soxhlet extraction is often required to get pure compounds. The simplified procedure developed by Lloyd-Jones³⁵ using potassium fluoride and tartaric acid was here followed to access analytically pure potassium ferrocenyltrifluoroborate (**19**) in 47% yield without purification (Scheme 3).



Scheme 3. Synthesis of potassium ferrocenyltrifluoroborate (**19**).

Triolborates are easily accessible by following Yamamoto and Miyaura's protocol.²⁷ Here, the reaction between **1** and 1,1,1-tris(hydroxymethyl)ethane under azeotropic removal of water afforded the ester **24**, which was directly converted into the triolborate **20** in the presence of potassium hydroxide in 70% yield over two steps (Scheme 4, top).

MIDA boronates, introduced by Mancilla³⁶ and nicely exploited in iterative cross-couplings by Burke, are prepared by reacting boronic acids and *N*-methyliminodiacetic acid. According to a literature procedure,^{28a} the new *N*-methyliminodiacetic acid boronate FcB(MIDA) (**21**) was obtained in 65% yield (Scheme 4, bottom).



Scheme 4. Synthesis of FcB(triolborate) (**20**) and FcB(MIDA) (**21**).

NMR spectroscopic characterization. All the new compounds were characterized by ¹¹B, ¹H and ¹³C NMR spectroscopy and, when possible, spectra were attributed on the basis of short and long range correlations (Figure 3).

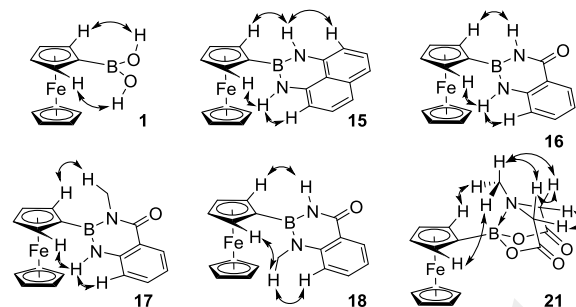


Figure 3. Selected NOESY correlations.

¹¹B NMR is a powerful tool to investigate the geometry and electronic environment around the heteroatom. As expected, upon quaternarization to the potassium trifluoroborate and triolborate, the ¹¹B NMR resonance is shifted to higher fields (**19**: δ(¹¹B) = 3.0 ppm, **20**: δ(¹¹B) = 2.4 ppm). The MIDA boronate **21** is characterized by a chemical shift of 13.9 ppm, consistent with the presence of a dative N-B bond at the pyramidalized boronate ester.^{28a} The chemical shifts of FcB(dan) and the three FcB(aam) are slightly shifted downfield (**15**: δ(¹¹B) = 32.4 ppm, **16**: δ(¹¹B) = 31.7 ppm, **17**: δ(¹¹B) = 31.9 ppm, **18**: δ(¹¹B) = 31.7 ppm) when compared to **1**. If the downfield shift from boronic acid to aminoboranes is known in the literature,³⁷ the difference between **15** and **16** is counterintuitive. Indeed, Nöth has reported that high δ(¹⁴N) results in high δ(¹¹B) on boronamides.³⁸ With higher ¹⁴N chemical shifts observed for the anthranilamide when compared to the diamionaphthalene,³⁹ one might have expected higher δ(¹¹B) in **16**. However, as revealed by X-ray diffraction analysis, the B(dan) substituent is tilted relative to the substituted cyclopentadienyl (Cp) ring (Figure 4) whereas boron anthranilamide is almost coplanar (Figure 5). Therefore, although weak, interaction between the vacant boron p-orbital and the ferrocenyl core could exist at a higher level in **16** than for **15**, leading to this unexpected ¹¹B chemical shifts reverse order. Very small differences in δ(¹¹B) are observed between **16**, **17** and **18** although the B(Me-aam) substituents are tilted in the two latter (Figures 6 and 7). Therefore, the electron-rich methyl group seems to counterbalance the reduced filling of boron p-orbital by the ferrocenyl group.

The ¹H and ¹³C spectra can help classify the borylated substituents in terms of electron-donating and -withdrawing properties when compared to reference compounds (Table 3).⁴⁰ Indeed, on monosubstituted ferrocenes, electron-withdrawing groups have a higher downshifting effect on H_α (adjacent to the substituent) than on H_β (remote to the substituent).

From ferrocene (FcH) to ferrocenylboronic acid (**1**), both H_α and slightly shift downfield (about 0.1 ppm), indicating weak electron-withdrawing properties for the B(OH)₂ substituent.

The electron-withdrawing properties of B(dan) and B(aam) groups are clearly established by the large chemical shifts observed (**15**: +0.55, **16**: +0.69 ppm for H_α and **15**: +0.23, **16**: +0.28 ppm for H_β), very similar to those of ketones (FcCOMe: +0.61 ppm for H_α and +0.28 ppm for H_β). Furthermore, the electron-withdrawing ability of the anthranilamide moiety can be modulated by the addition of methyl groups (**16**: +0.69, **17**: +0.53, **18**: +0.55 ppm for H_α), opening possibilities for the tuning of boron Lewis acidic character. The B(MIDA) group (**21**) is closer to the weak electron-withdrawing group SiMe₃.⁴¹

Table 3. Selected ^1H , ^{13}C and ^{11}B NMR spectroscopic data.

Compound	δ (ppm)							
	H_α	H_β	C ρ	C_{ipso}	C_α	C_β	C ρ	B
FcH^a	4.17	4.17	4.17	67.7	67.7	67.7	67.7	nd
1^a	4.28	4.29	4.05	/ ^d	74.2	72.4	69.2	31.0
15^a	4.72	4.40	4.12	/ ^d	72.1	71.0	68.3	32.4
16^a	4.86	4.45	4.07	/ ^d	73.1	72.3	68.9	31.7
17^a	4.70	4.54	4.15	/ ^d	73.9	71.6	68.4	31.9
18^a	4.72	4.51	4.16	/ ^d	74.7	72.1	69.1	31.7
19^a	3.87	3.87	3.96	/ ^d	71.1 ^c	66.9 ^c	67.2	3.0
20^a	3.85	3.79 ^c	3.98 ^c	/ ^d	71.6 ^c	66.5	67.3	2.4
21^a	4.08	4.27	4.17	/ ^d	71.6	70.1	68.2	13.9
FcNH₂	4.02 ^b	3.87 ^b	4.12 ^b	104.2 ^e	58.8 ^e	63.0 ^e	/ ^e	nd
FcTMS^a	4.12	4.35	4.14	71.0	72.4	70.4	67.8	nd
FcCOMe^a	4.78	4.56	4.24	79.2	69.2	71.9	69.5	nd
FcPPh₂^b	4.07	4.33	4.04	nd	nd	nd	nd	nd

^a In DMSO- d_6 . ^b From ref ^{40d}, spectra recorded in CDCl_3 . ^c Tentative assignment based on chemical shifts. ^d C_{ipso} not seen due to boron quadrupolar coupling. ^e From ref ^{40c}. nd: not determined.

As expected, the trifluoroborate **19** and triolborate **20** act as electron-donating groups. They appear as powerful as the amino group with an almost similar enrichment of both α and β positions (**19**: - 0.30, **20**: - 0.32 ppm for H_α and **19**: - 0.30, **20**: - 0.38 ppm for H_β).

It is known that functional groups have little effect onto the unsubstituted Cp ring.^{40d} However, small to moderate downfield shifts are generally observed for electron-withdrawing groups whereas small upfield shifts take place with electron-donating groups. The effect of the borylated groups used in this study are therefore difficult to rationalize. Indeed, $\text{B}(\text{OH})_2$, $\text{B}(\text{dan})$ and $\text{B}(\text{aam})$ groups, classified as electron-withdrawing based on ^{11}B NMR, all shift upfield the ^1H NMR signal of the Cp ring. Furthermore, their effect is more pronounced than an amino and close to that of a phosphino substituent. The remaining boron-anthranilamides (**17**, **18**) have very little upfield shifting effect. Although the origin of these results remains unclear, this might results from the variable degree of interaction between the ferrocenyl core and the boron vacant p-orbital. On the other hand, the trifluoroborate (**19**) and triolborate (**20**) both act as strong electron-donating as judged by the high upfield shifts of the Cp ring whereas the MIDA boronate (**21**) group has no effect.

Concerning ^{13}C NMR spectroscopy, C_β are known to be more sensitive to strong electron-withdrawing group whereas C_α are more influenced by strong electron-donating substituents.^{40a, 40c} For medium electron-donating and -withdrawing groups, chemical shifts are more difficult to classify. Indeed, although ^{13}C chemical shifts observed for $\text{B}(\text{OH})_2$ suggest an electron-donating group, this might not be representative as we previously classified this group as a weak electron-withdrawing group. A similar contradiction is noted for $\text{B}(\text{MIDA})$ (**21**): ^1H chemical shifts suggest an electron-withdrawing group whereas ^{13}C chemical shifts are closer to an electron-donating group behavior. Therefore, the unambiguous classification of these groups cannot be done only with ^1H and ^{13}C spectroscopy.

Results were more intriguing for $\text{B}(\text{dan})$ (**15**) and $\text{B}(\text{aam})$ (**16-18**), all classified as electron-withdrawing groups from ^1H NMR data. Therefore, their shifting effect on the C_β should be higher than on C_α . However, the opposite effect was recorded. A surprising slight increase in the short-range acidifying effect

is also noted on C_α from **16** to **18**. A similar effect was also noted by Wrackmeyer and Herberhold on bis(diisopropylamino)boryl ferrocene and remains unexplained.⁴² On the contrary, the higher shifts observed for C_α compared to C_β on trifluoroborate (**19**), triolborate (**20**) are in agreement with the literature.

Minor variations of the unsubstituted Cp ring were also noted. Its ^{13}C resonance is shifted upfield for the two borates (**19**: $\delta(^{13}\text{C}) = - 0.5$ ppm, **20**: $\delta(^{13}\text{C}) = - 0.4$ ppm). On the contrary, the ^{13}C resonance of the Cp is shifted downfield for $\text{FcB}(\text{OH})_2$ (**1**), $\text{FcB}(\text{aam})$ (**16**), $\text{FcB}(\text{dan})$ (**15**) and $\text{FcB}(\text{MIDA})$ (**21**) ($\delta(^{13}\text{C}) = + 1.50, + 1.20, + 0.60, + 0.50$ ppm, respectively). Interestingly, this order correlates with the boron chemical shifts for the trivalent derivatives (**1**: $\delta(^{11}\text{B}) = 31.0$ ppm, **16**: $\delta(^{11}\text{B}) = 31.7$ ppm, **15**: $\delta(^{11}\text{B}) = 32.4$ ppm). Therefore, as the donation of the boron substituents into the boron vacant p orbital increases, boron Lewis acidity decreases and the unsubstituted Cp ring is less electron-depleted. This suggests interactions between boron, C_{ipso} and iron atoms or through-space interactions between boron and the unsubstituted Cp, as proposed by Holthausen and Wagner.⁴³ As variations of interatomic distances and bending angles are characteristic of such interactions, we next study the structure of the borylated ferrocenes by X-ray crystallography.

X-ray crystal structure determination. Crystals of **15**, **16**, **17**, **18**, **19** and **21** were obtained by evaporation of their corresponding solutions.

In **15**, the planar diaminonaphthalene group is tilted relative to the substituted Cp ring (Figure 4, $\text{C}_6\text{-C}_{10}\text{-B}_{11}\text{-N}_{22} = 16.5(3)^\circ$), whereas the Cp and anthranilamide rings are almost coplanar in **16** (Figure 5, $\text{C}_6\text{-C}_{10}\text{-B}_{11}\text{-N}_{12} = 0.9(3)^\circ$). However, the introduction of the methyl group in **17** and **18** forces the borylated substituent to rotate and release the steric pressure generated by this additional substituent (Figures 6 and 7, **17**: $\text{C}_6\text{-C}_{10}\text{-B}_{11}\text{-N}_{22} = 30.1(5)^\circ$, **18**: $\text{C}_6\text{-C}_{10}\text{-B}_{11}\text{-N}_{22} = 31.7(4)^\circ$).

The $\text{C}_{\text{ipso}}\text{-B}$ bonds are almost similar in **15** and **16** (**15**: $\text{C}_{10}\text{-B}_{11}$ 1.545(3) Å, **16**: $\text{C}_{10}\text{-B}_{11}$ 1.541(2) Å), whereas they appear slightly longer in the methylated derivatives (**17** and **18**: 1.554(3-5) Å). On the contrary, the Fe-B distance increases from **16** to **15** to **17** and **18** (**16**: $\text{Fe}_1\text{-B}_{11}$ 3.1074(18) Å, **15**: $\text{Fe}_1\text{-B}_{11}$ 3.1695(19) Å, **17**: $\text{Fe}_1\text{-B}_{11}$ 3.228(4) Å, **18**: $\text{Fe}_1\text{-B}_{11}$ 3.232(3) Å). The bending of the boron substituent toward the iron atom

in these compounds is highly significant and is evaluated by the angle α^* between the center of gravity of the substituted Cp ring, the C_{ipso} and the boron atom. According to the crystallographic data, it is the highest in **16** and decreases upon introduction of the methyl groups, whereas they are similar for **15** and **17** (**15**: 5.53°, **16**: 7.97°, **17**: 5.50°, **18**: 1.08°). These data suggest less interactions between the ferrocenyl group and boron in **15** compared to **16**, resulting from the higher filling of the boron empty orbital by the nitrogen lone pairs in **15**. This might reflect the intrinsic electronic differences between the aniline and the amide. The methyl group has a similar donating effect in **17** and **18**, although clearly higher for the latter, probably for similar reasons. This is in agreement with the work of Wagner⁴³ in which high angles α^* are observed with strong Lewis acidic boron substituents. With angles between BBr₂ and B(OH)₂, the boron naphthalene-1,8-diamido **15** and the two boron-anthranilamides **16** and **17** show moderate Lewis acidity character. Only **18**, as a result of the methylated aniline, features a decrease in its Lewis acidic character.

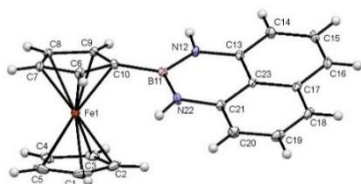


Figure 4. Molecular structure of compound **15**; thermal ellipsoids shown at the 30% probability level. Selected bond lengths [Å], and angles [°]: Fe1-B11 3.1695(19), C10-B11 1.545(3), B11-N12 1.423(3), B11-N22 1.423(3), α^* = 5.53, C₆-C10-B11-N22 = 16.5(3).

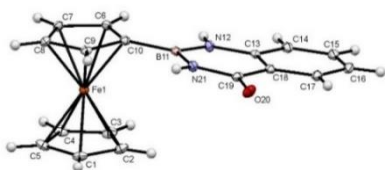


Figure 5. Molecular structure of compound **16**; thermal ellipsoids shown at the 30% probability level. Selected bond lengths [Å] and angles [°]: Fe1-B11 3.1074(18), C10-B11 1.541(2), B11-N12 1.420(2), B11-N21 1.442(2), α^* = 7.97, C₆-C10-B11-N12 = 0.9(3).

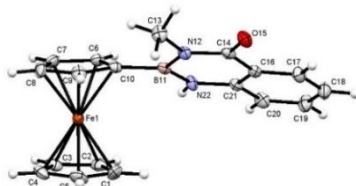


Figure 6. Molecular structure of compound **17**; thermal ellipsoids shown at the 30% probability level. Selected bond lengths [Å] and angles [°]: Fe1-B11 3.228(4), C10-B11 1.554(5), B11-N12 1.452(5), B11-N22 1.406(5), α^* = 5.50, C₆-C10-B11-N22 = 30.1(5).

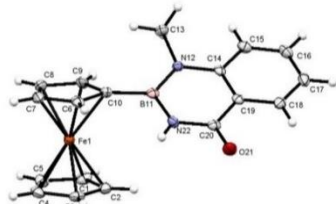


Figure 7. Molecular structure of compound **18**; thermal ellipsoids shown at the 30% probability level. Selected bond lengths [Å] and

angles [°]: Fe1-B11 3.232(3), C10-B11 1.554(3), B11-N12 1.425(3), B11-N22 1.438(3), α^* = 1.08, C₆-C10-B11-N22 = 31.7(4).

The crystal structure of **19** reveals the longest bond between boron and cyclopentadienyl ring (Figure 8, C₁₀-B₁₁ 1.588(4) Å), as well as the smallest bending angle (α^* 0.98°). These values are in good agreement with the reported X-ray crystal structures of the FcBF₃⁻ anion and are characteristic of quaternarized boron atom.^{16, 18} However, unlike the reported structures of ferrocenyltrifluoroborate anions, the role of the potassium cation in the crystal packing should be pointed out (Figure 8). Indeed, each potassium ion is shared between three BF₃ groups and therefore participates to the formation of an inner cationic layer while the ferrocene parts are pointing outward, as observed for unsubstituted potassium phenyltrifluoroborate.⁴⁴

FcB(MIDA) (**21**) has its iron-boron distance (Fe₁-B₁₁: 3.1695(19) Å), C_{ipso}-B bond (C₁₀-B₁₁: 1.568(2) Å) and bend angle (α^* 3.17°) between those of FcB(OH)₂ (**1**) and FcBF₃K (**19**), which confirm the moderate electron-donating properties of this substituent. The single-crystal X-ray diffraction data also confirm the presence of a dative nitrogen-boron bond (B₁₁-N₁₂ 1.664(2) Å). When compared to other heterocyclic B(MIDA) derivatives such as the 2-pyridine,⁴⁵ 2-pyrazine and 5-thiazole ones,⁴⁶ it appears that the C_{ipso}-B bond is shorter (from -0.016 to -0.021 Å) while the B-N dative bond is longer (from +0.016 to +0.030 Å) in **21**. This longer dative bond results from the better electronic donation of the ferrocenyl core to boron.

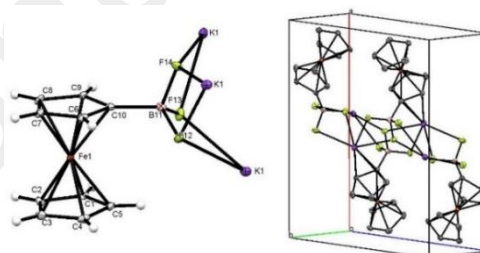


Figure 8. Left: molecular structure of compound **19**; thermal ellipsoids shown at the 30% probability level. Selected bond lengths [Å] and angles [°]: Fe1-B11 3.272(3), C10-B11 1.588(4), B11-F12 1.417(4), B11-F13 1.420(4), B11-F14 1.440(3), α^* = 0.98. Right: Arrangement of the molecules at the solid state (atom color: K, violet; F, green; B, pink; C, grey; Fe, orange). Hydrogen were omitted for clarity.

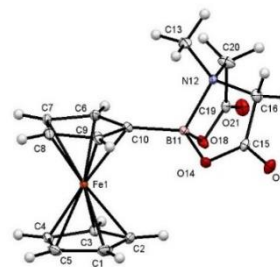


Figure 9. Molecular structure of compound **21**; thermal ellipsoids shown at the 30% probability level. Selected bond lengths [Å] and angles [°] and torsion angles [°]: Fe1-B11 3.1695(19), C10-B11 1.568(2), B11-O14 1.476(2), B11-O18 1.490(2), B11-N12 1.664(2), α^* = 3.17.

Electrochemistry.

The electrochemical behavior of ferrocenboronic acid and its derivatives was next studied by cyclic voltammetry (Table 4). Due to the low solubility of these complexes in acetonitrile,

the measurements were performed in dry, oxygen-free dimethylformamide (DMF) at a concentration of 3 mM with *n*Bu₄NPF₆ (0.1 M) as supporting electrolyte. For comparison, the cyclic voltammogram of ferrocene (**Fc**) was recorded in the same solvent and displayed a reversible mono-electronic system with a peak separation of 80 mV.

Table 4. Electrochemical Data^a

Compound	E_{pa} (V)	E_{pc} (V)	i_{pa}/i_{pc}	ΔE (mV)
Fc	0.57	0.49	0.97	–
1	0.56	0.38	0.97	10
15	0.58	0.41	nr	–10
16	0.62	0.54	0.97	–50
17	0.61	0.53	0.97	–40
18	0.60	0.51	1.20	–30
19	0.26	0.18	1.06	310
20	0.60	0.52 ^b	nr	–30
21	0.55	0.47	0.97	20

^a Scan rate = 0.1 V/s. Bu₄NPF₆ (0.1 M) in DMF; working electrode: glassy carbon; reference electrode: Ag/AgCl. ^b An additional oxidation peak was observed at 0.16 V. nr: not reversible. Potential differences, ΔE (defined as $E_{pa}^{Fc} - E_{pa}^{boronic}$).

Compounds **1**, **16**, **17**, **19** and **21** exhibited typical one-electron and reversible processes at a scan rate of 0.1 V/s with the i_{pc}/i_{pa} ratios of unity and the peak separation in the 80–90 mV range. As a result, the corresponding ferricinium species appeared stable at the time scale of cyclic voltammetry.

The easier oxidation peak for compound **19** was easily attributed to the presence of the trifluoroborate substituent. Obviously, quaternarization of the boron substituent provided a significant cathodic shift ($E_{pa}^{Fc} - E_{pa}^{19} = 310$ mV) and this observation is in agreement with that of Grzybowski.¹⁹ One might expect a similar observation for the triolborate **20**. Unfortunately, the voltammogram of **20** displayed a first irreversible oxidation peak ($E_{pa1} = 0.16$), which may be attributed to a chemical reaction giving rise to a new reversible oxidation system at $E_{pa1} = 0.60$ V. The origin of this chemical process remains unclear even if the second system could be related to the reversible Fe^{2+}/Fe^{3+} process. The exact nature of this follow-up chemical reaction would require further investigation.

We also reasoned that introduction of the B(MIDA) moiety onto ferrocene would increase significantly its oxidation potential due to the ester functionalities. However, for compound **21**, a fully reversible couple ($i_{pa}/i_{pc} = 0.97$) was observed, indicating that the nitrogen donation into the vacant boron p-orbital can counterbalance the electron-withdrawing properties of the carbonyl function. Finally, from boronic acid (**1**) to boron complexes **16**, **17** and **18**, the potential at which oxidation occurs results from the moderate electron-withdrawing properties of the anthranilamide group. Conversely, the cyclic voltammogram of complex **18** exhibited an i_{pa}/i_{pc} value of 1.20, which is in agreement with a partial loss of reversibility. This phenomenon could be attributed to a slow electron exchange between the ferricinium moiety and the *N*-methyl group of the anthranilamide substituent. Hence, the presence of an alkyl substituted nitrogen atom may be detrimental to the stability of the ferrocenium species.

The electrochemical behavior of complex **15** is worthy of an additional comment. Indeed, its cyclic voltammogram exhibits an irreversible oxidation peak at $E_{pa} = 0.58$ V, whose height is twice than that recorded for the vast majority of the substrates. This abnormal result may be attributed to the oxidation of both

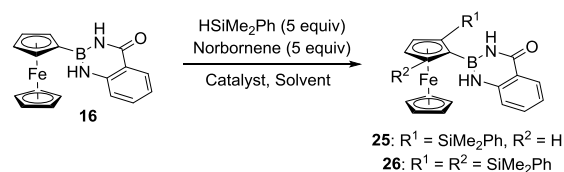
the ferrocene and 1,8-diaminonaphthalene core, which occurs at a very similar potential. To confirm this hypothesis, the anodic electrochemistry of 1,8-diaminonaphthalene displayed an irreversible single system at $E_{pa} = 0.6$ V vs Ag/AgCl (see SI). Therefore, the oxidation potential of 1,8-diaminonaphthalene is approximately the same than that recorded for the ferrocene itself.

Catalytic C-H activation.

In recent years, the silylation of unactivated C-H bond has enormously grown with the development of efficient catalytic systems.⁴⁷ Nowadays, the directed intermolecular silylation is an appealing way to access silylated aromatics in a site-selective fashion. Various directing groups can be used and, in 2009 and 2011, Suginome reported the ability of borylated 2-(5-pyrazolyl)aniline (pza) and anthranilamide (aam) to direct the ortho-silylation of substituted benzenes.^{26, 48} However, to the best of our knowledge, silylated ferrocenes have only been prepared by interception of lithiated ferrocenes and the catalytic silylation of ferrocenes has never been reported.⁴⁹

Here, we present preliminary results on the use of B(aam) to direct ferrocene C-H bonds activation. We initially surveyed the reaction of **16** with HSiMe₂Ph in the presence of norbornene as hydrogen acceptor and [Ir(OMe)(COD)]₂/4,4'-di-*tert*-butyl-[2,2']bipyridinyl (dtbpy) as catalytic system.⁵⁰ To our delight, the product **25** was formed, albeit in very low yield (Table 5, entry 1). We therefore switched to Suginome's conditions²⁶ and isolated the title product in a better yield (entry 2). By doubling the catalyst loading, we obtained **25** in a moderate yield, together with a small amount of the bis-silylated derivative **26** (entry 3). Interestingly, when the reaction time was extended, the mono-/bisfunctionalized products ratio changed and **26** was isolated in 48% yield (entry 4).

Table 5. Study of FcB(aam) silylation.



Entry	Conditions	25 (%)	26 (%)
1	[Ir(OMe)(COD)] ₂ (3 mol%), dtbpy (6 mol%), Octane, 126 °C, 20 h	10	nd
2	RuH ₂ (CO)(PPh ₃) ₃ (6 mol%), Toluene, 135 °C, 21 h	20	nd
3	RuH ₂ (CO)(PPh ₃) ₃ (12 mol%), Toluene, 135 °C, 21 h	50	26
4	RuH ₂ (CO)(PPh ₃) ₃ (12 mol%), Toluene, 135 °C, 44 h	19	48

Silylation was also attempted from the methylated anthranilamides **17** and **18**; however, their instability during both reaction and purification steps led to multiple products.

The conformation of the two substituents in **25** was elucidated by 2-dimensional NMR experiments and X-ray diffraction analysis (Figure 10). From NOESY experiments, the correlations seen between the amide proton and the unsubstituted Cp ring suggest that the amide is pointing down. Correlations observed between the aniline NH and one of the methyl of the SiMe₂Ph group also support this orientation. Interestingly, the correlations observed between the dimethylsilyl group and both the NH and the ferrocenyl proton suggests some degree of free rotation between the C_{ipso}-B and C_{ipso}-Si bounds. The structure at the solid state confirms the NMR analysis (Figure 9, right).

The amide proton is clearly oriented toward the unsubstituted Cp ring while the phenyl ring of the silylated substituent is pointing up, explaining the absence of correlation of any NH and phenyl protons. It is noteworthy that the introduction of the dimethylphenylsilyl group has a clear effect on the borylated substituent. From **16** to **25**, both the C6-B11 and Fe1-B11 distances increase (+0.016 Å and +0.184 Å, respectively), while the bending angle α^* decreases (-4.83°). This indicates lower interactions between boron, C_{ipso} and iron atoms, resulting from the steric repulsion generated by the silylated group.

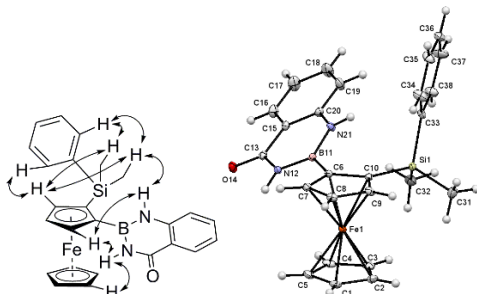


Figure 10. Left: selected NOESY correlations seen in **25**. Right: molecular structure of compound **25**; thermal ellipsoids shown at the 30% probability level. Selected bond lengths [Å] and angles [°]: Fe1-B11 3.292(2), C6-B11 1.557(3), B11-N21 1.416(3), B11-N12 1.441(3), C10-Si1 1.866(2), $\alpha^*(\text{C10-B11}) = 3.14$, $\alpha^*(\text{C10-Si1}) = 4.42$.

Due to the steric hindrance resulting from the two silylated groups, the borylated substituent in **26** should be almost perpendicular to the Cp ring. However, despite all our efforts, crystals suitable for X-ray diffraction analysis were never obtained. However, NOESY experiment revealed correlations of both NH with the unsubstituted Cp ring, thus suggesting two conformers, one with the amide pointing toward the unsubstituted Cp ring and one with the amide pointing up.

Encouraged by these promising results in silylation, we finally turned our attention to the borylation of ferrocene C-H bond, directed by the boron-anthranilamide group. If successful, this would constitute the first ortho-directed C-H borylation of ferrocene C-H bonds. Indeed, to the best of our knowledge, the catalytic ferrocene borylation has only been reported twice, one by Plenio,⁵¹ affording 1,3-disubstituted derivatives, and the second by Li,⁵² only dedicated to the formation of monosubstituted products. Rhodium-catalyzed borylation was first evaluated. However, despite all our efforts, multiple products were invariably formed (Table 6, entries 1 and 2). Surprisingly, the use of Plenio's conditions afforded **28** as the main product, resulting from the directing group functionalization (entries 3 and 4). Such a regioselectivity switch between catalytic rhodium-catalyzed silylation and iridium-catalyzed borylation is known,⁵³ and was also recently documented in the benzene series using the same boron anthranilamide directing group.⁵⁴ However, even if it is known that borylation is sensitive to ortho substituents, the exact origin of this reversal is not totally understood.⁵⁵ Taking into account the generally accepted mechanism of iridium-catalyzed borylation,⁵⁵ this might indicate that the directing group would not be effective to coordinate the iridium catalyst surrounded by three pinacol residues and the bipyridine ligand. To open a coordination site onto the metal, we therefore tested the hemilabile ligand designed by Lassaletta.⁵⁶ However, whatever the conditions used, **28** was always isolated as the main product, although in considerably lower yield (entry 5).

Table 6. Study of FcB(aam) borylation.

Entry	Conditions	27 (%)	28 (%)
1	RuH ₂ (CO)(PPh ₃) ₃ (12 mol%), B ₂ Pin ₂ (5.0 equiv) Toluene, 135 °C, 21 h	nd	nd
2	RuH ₂ (CO)(PPh ₃) ₃ (12 mol%), HBPin (5.0 equiv) Toluene, 135 °C, 21 h	nd	nd
3	[Ir(OMe)(COD)] ₂ (3 mol%), dtbpy (6 mol%), B ₂ Pin ₂ (0.5 equiv), Octane, 126 °C, 20 h	nd	8
4	[Ir(OMe)(COD)] ₂ (1.5 mol%), dtbpy (3 mol%), B ₂ Pin ₂ (1.0 equiv), Octane, 126 °C, 20 h	nd	25
5	[Ir(OMe)(COD)] ₂ (3 mol%), L1 (6 mol%), B ₂ Pin ₂ (1.0 equiv), Octane, 126 °C, 20 h	nd	7

Taking into account the low yield of silylated product **25** formed and the absence of ferrocene borylation, both under iridium catalysis, it can be advanced that the boron-anthranilamide group has poor ortho-directing ability for this metal. The borylation site is also interesting as one could expect a reaction either at the most acidic (next to the carbonyl) or at the less hindered positions. However, extensive NMR and X-ray diffraction analysis proved without any doubt the structure (Figure 11), which features both intra- and intermolecular hydrogen bonds.

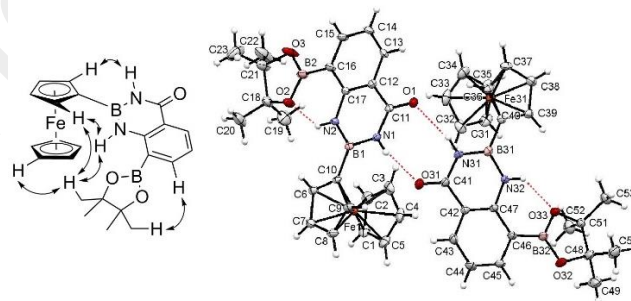
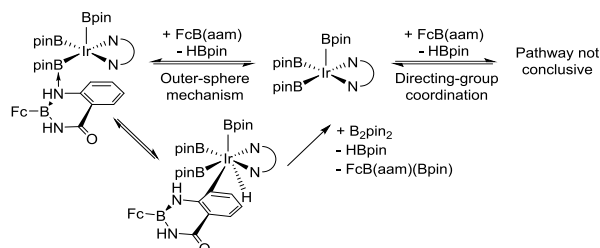


Figure 11. Left: selected NOESY correlations seen in **28**. Right: Molecular structure of compound **28**; thermal ellipsoids shown at the 30% probability level. Selected bond lengths [Å] and angles [°]: Fe1-B1 3.121(3), C10-B1 1.546(4), B1-N1 1.437(4), B1-N2 1.420(4), O1-H31N 2.1275, O31-H1N 2.1183, O2-H2N 2.1153, O33-H32N 2.1625, Fe31-B31 3.161(4), C40-B31 1.553(5), B31-N31 1.440(4), B31-N32 1.421(4), $\alpha^*(\text{C10-B1}) = 5.84$. Hydrogen bonds indicated in dotted red lines.

The directing group functionalization gave clues about the different mechanisms operating for rhodium-catalyzed silylation and iridium-catalyzed borylation. Indeed, from the work of Suginome,²⁶ free amide NH is required to direct the rhodium-catalyzed silylation whereas the aniline does not appear to participate. However, the regioselectivity here observed for the iridium-catalyzed borylation is closer to the work of Maleczka and Smith on the borylation of indoles in which the direct interaction of the indole nitrogen and iridium center, as well as an outer-sphere mechanism involving the nitrogen and the vacant p-orbital of a boryl ligand, have been proposed.^{55, 57} In an attempt to rationalize our results, the sterically accessible (especially bearing labile monophosphine) rhodium catalytic active

species might interact with the amide to perform the ferrocene C-H bond activation as planned. However, the iridium catalyst might not be able to interact with this boronamide, for electronic or steric reasons, and an outer-sphere mechanism would therefore become preferable as depicted in Scheme 5. The better lone-pair donating properties of anilines, when compared to amides, could explain this site of functionalization, whereas the interaction between the aniline nitrogen and the vacant p-orbital of the boron, decreasing the stability of such intermediate, would explain why our regiocontrol and yield are lower than those observed by Maleckza and Smith.



Scheme 5. Putative mechanism of regioselectivity switch during borylation of **16**.

CONCLUSION

In summary, we prepared seven original ferroceneboronic acid derivatives bearing borylated groups relevant in cross-coupling reactions or as ortho-directing groups. NMR, electrochemical and X-ray diffraction analysis helped establish a general overview of the structural and electronic behavior of these derivatives and to classify them in terms of electron-withdrawing or -donating properties. Moreover, preliminary results showed the ability of boron anthranilamide to direct the rhodium-catalyzed ferrocenic C-H bond activation. Studies are at present ongoing to establish the limits of this methodology, especially in its enantioselective version. Finally, we have reported on original regioselectivity switch during an iridium-catalyzed borylation, which resulted in the functionalization of the boron anthranilamide group. A putative outer-sphere mechanism was proposed to account of the experimental results and additional investigations are ongoing to uncover the key parameters controlling this unexpected transformation. Therefore, it should be pointed out the marked differences between ferrocene and benzene, during both the synthesis of these borylated derivatives and their use in catalytic transformation.

ASSOCIATED CONTENT

Supporting Information

The Supporting Information is available free of charge on the ACS Publications website at DOI: 10.1021/acs.organomet.XXX.

Experimental procedures, compounds analyses,
X-ray crystallographic details, NMR spectra, cyclic voltammograms (PDF)
Crystallographic data (CIF)

Accession Codes

CCDC 1853253-1853260. The crystallographic data can be obtained free of charge via www.ccdc.cam.ac.uk/data_request/cif, or by emailing data_request@ccdc.cam.ac.uk, or by contacting The Cambridge Crystallographic Data Centre, 12 Union Road, Cambridge CB2 1EZ, UK; fax: +44 1223 336033.

AUTHOR INFORMATION

Corresponding Author

* E-mail for W.E.: william.erb@univ-rennes1.fr.

ORCID

William Erb: 0000-0002-2906-2091

Thierry Roisnel: 0000-0002-6088-4472

Vincent Dorcet: 0000-0001-9423-995X

Notes

The authors declare no competing financial interest.

ACKNOWLEDGMENTS

This work was supported by the Université de Rennes 1. We acknowledge the Fonds Européen de Développement Régional (FEDER; D8 VENTURE Bruker AXS diffractometer). W.E. would like to thank Dr. B. Carboni for the generous gift of MIDA and Prof. F. Mongin for critically reviewing this document and making valuable suggestions.

REFERENCES

1. *Ferrocenes: Homogeneous Catalysis, Organic Synthesis, Materials Science*, A. Togni, T. H., Ed. VCH: Weinheim, **2008**.
2. (a) *Ferrocenes: Ligands, Materials and Biomolecules*, Štěpnička, P., Ed. Wiley: Chichester, **2008**; (b) Top, S.; Tang, J.; Vessieres, A.; Carrez, D.; Provot, C.; Jaouen, G. Ferrocenyl hydroxytamoxifen: a prototype for a new range of oestradiol receptor site-directed cytotoxics. *Chem. Commun.* **1996**, 955-956; (c) Biot, C.; Glorian, G.; Maciejewski, L. A.; Brocard, J. S.; Domarle, O.; Blampain, G.; Millet, P.; Georges, A. J.; Abessolo, H.; Dive, D.; Lebibi, J. Synthesis and Antimalarial Activity in Vitro and in Vivo of a New Ferrocene-Chloroquine Analogue. *J. Med. Chem.* **1997**, *40*, 3715-3718; (d) Pinto, A.; Hoffmanns, U.; Ott, M.; Fricker, G.; Metzler-Nolte, N. Modification with Organometallic Compounds Improves Crossing of the Blood-Brain Barrier of [Leu5]-Enkephalin Derivatives in an In Vitro Model System. *ChemBioChem* **2009**, *10*, 1852-1860.
3. Toma, Š.; Šebesta, R. Applications of Ferrocenium Salts in Organic Synthesis. *Synthesis* **2015**, *47*, 1683-1695.
4. (a) Khobragade, D. A.; Mahamulkar, S. G.; Pospíšil, L.; Čisářová, I.; Rulišek, L.; Jahn, U. Acceptor-Substituted Ferrocenium Salts as Strong, Single-Electron Oxidants: Synthesis, Electrochemistry, Theoretical Investigations, and Initial Synthetic Application. *Chem. Eur. J.* **2012**, *18*, 12267-12277; (b) Mo, X.; Yakiwchuk, J.; Dansereau, J.; McCubbin, J. A.; Hall, D. G. Unsymmetrical Diarylmethanes by Ferroceniumboronic Acid Catalyzed Direct Friedel-Crafts Reactions with Deactivated Benzylic Alcohols: Enhanced Reactivity due to Ion-Pairing Effects. *J. Am. Chem. Soc.* **2015**, *137*, 9694-9703; (c) Mo, X.; Hall, D. G. Dual Catalysis Using Boronic Acid and Chiral Amine: Acyclic Quaternary Carbons via Enantioselective Alkylation of Branched Aldehydes with Allylic Alcohols. *J. Am. Chem. Soc.* **2016**, *138*, 10762-10765.
5. (a) Tazi, M.; Erb, W.; Halauko, Y. S.; Ivashkevich, O. A.; Matulis, V. E.; Roisnel, T.; Dorcet, V.; Mongin, F. From 2- to 3-Substituted Ferrocene Carboxamides or How to Apply Halogen "Dance" to the Ferrocene Series. *Organometallics* **2017**, *36*, 4770-4778; (b) Erb, W.; Levanen, G.; Roisnel, T.; Dorcet, V. Application of the Curtius rearrangement to the synthesis of 1'-aminoferrocene-1-carboxylic acid derivatives. *New J. Chem.* **2018**, *42*, 3808-3818; (c) Tazi, M.; Hedidi, M.; Erb, W.; Halauko, Y. S.; Ivashkevich, O. A.; Matulis, V. E.; Roisnel, T.; Dorcet, V.; Bentabed-Ababsa, G.; Mongin, F. Fluoro- and Chloroferrocene: From 2- to 3-Substituted Derivatives. *Organometallics* **2018**, *37*, 2207-2211; (d) Nayyar, B.; Kapoor, R.; Lutter, M.; Alnasr, H.; Jurkschat, K. It's Getting Tight: Highly Substituted Intramolecularly P=O-Sn Coordinated Ferrocene Derivatives. *Eur.*

- J. Inorg. Chem.* **2017**, *2017*, 3967-3978; (e) Nayyar, B.; Koop, S.; Lutter, M.; Jurkschat, K. Ferrocene-Based, Potentially D,C,D- Coordinating (D = O, S), Pincer-Type Proligands and Their Organotin Derivatives. *Eur. J. Inorg. Chem.* **2017**, *2017*, 3233-3238; (f) Záborský, M.; Císařová, I.; Štěpnička, P. Synthesis, Coordination, and Catalytic Use of 1'-(Diphenylphosphino)ferrocene-1-sulfonate Anion. *Organometallics* **2018**, *37*, 1615-1626; (g) Korb, M.; Lang, H. Planar Chirality from the Chiral Pool: Diastereoselective Anionic Phospho-Fries Rearrangements at Ferrocene. *Organometallics* **2014**, *33*, 6643-6659; (h) Tagne Kuate, A. C.; Lalancette, R. A.; Jákľe, F. Planar-chiral ferrocenylphosphine-borane complexes featuring agostic-type B-H...E (E = Hg, Sn) interactions. *Dalton Trans.* **2017**, *46*, 6253-6264.
6. (a) Nesmeyanov, A. N., Sazonowa, V. A. & Drozd, V. N. *Dokl. Akad. Nauk SSSR* **1959**, *126*, 1004-1008; (b) Nesmejanow, A. N.; Ssasonowa, W. A.; Drosd, V. N. Synthese von Ferrocenderivaten mittels bor- und halogensubstituierter Ferrocene. *Chem. Ber.* **1960**, *93*, 2717-2729.
7. Shechter, H.; Helling, J. F. Ferrocenyl and 1,1'-Ferrocenylene Grignard Reagents. *J. Org. Chem.* **1961**, *26*, 1034-1037.
8. McVey, S.; Morrison, I. G.; Pauson, P. L. Ferrocene derivatives. Part XVII. The aminomethylation of methoxy- and dimethoxy-ferrocene. *J. Chem. Soc. C* **1967**, 1847-1850.
9. Post, E. W.; Cooks, R. G.; Kotz, J. C. Ferrocenylboranes. II. Ferrocenyl boric acids and related compounds. Mass spectral and hydrogen-bonding studies. *Inorg. Chem.* **1970**, *9*, 1670-1677.
10. Floris, B.; Illuminati, G. The kinetics and mechanism of the protodeboronation of ferroceneboronic acid in moderately concentrated sulfuric acid. *J. Organomet. Chem.* **1978**, *150*, 101-113.
11. S. Kamounah, F.; B. Christensen, J. A New Preparation of Iodoferrrocene. *J. Chem. Res. (S)* **1997**, 150-150.
12. Lacina, K.; Novotný, J.; Moravec, Z.; Skládal, P. Interaction of ferroceneboronic acid with diols at aqueous and non-aqueous conditions - signalling and binding abilities of an electrochemical probe for saccharides. *Electrochim. Acta* **2015**, *153*, 280-286.
13. Bresner, C.; Aldridge, S.; Fallis, I. A.; Ooi, L.-L. Hydrogen-bonding motifs in the solid-state structure of ferroceneboronic acid. *Acta Crystallogr. E* **2004**, *60*, m441-m443.
14. Voloshin, Y. Z.; Makarov, I. S.; Vologzhanina, A. V.; Monakov, Y. B.; Islamova, R. M.; Polshin, E. V.; Bubnov, Y. N. Template synthesis and structures of bis-ferrocenylboronate macrobicyclic iron(II) tris-dioximates. *Russ. Chem. Bull.* **2008**, *57*, 1223-1230.
15. (a) Darses, S.; Genet, J.-P. Potassium Organotrifluoroborates: New Perspectives in Organic Synthesis. *Chem. Rev.* **2008**, *108*, 288-325; (b) Molander, G. A.; Canturk, B. Organotrifluoroborates and Monocoordinated Palladium Complexes as Catalysts—A Perfect Combination for Suzuki–Miyaura Coupling. *Angew. Chem. Int. Ed.* **2009**, *48*, 9240-9261; (c) Molander, G. A. Organotrifluoroborates: Another Branch of the Mighty Oak. *J. Org. Chem.* **2015**, *80*, 7837-7848.
16. Quach, T. D.; Batey, R. A.; Lough, A. J. Tetra-*n*-butylammonium ferrocenyltrifluoroborate. *Acta Crystallogr. E* **2001**, *57*, m320-m321.
17. Bats, J. W.; Scheibitz, M.; Wagner, M. The twinned structure of ferricenytrifluoroborate. *Acta Crystallogr. C* **2003**, *59*, m355-m357.
18. Bresner, C.; Aldridge, S.; Fallis, I. A.; Jones, C.; Ooi, L.-L. Selective Electrochemical Detection of Hydrogen Fluoride by Amphiphilic Ferrocene Derivatives. *Angew. Chem. Int. Ed.* **2005**, *44*, 3606-3609.
19. Smith, P. F.; Korsan, J. M.; Grimm, T. R.; Grzybowski, J. J. Reaction of boronic acids with tetrafluoroborate? It depends on the acidity. *Inorg. Chem. Commun.* **2014**, *48*, 144-146.
20. (a) Bats, J. W.; Ma, K.; Wagner, M. Isomorphism and phase transition in triferrocenylboroxine and triferrocenylborazine. *Acta Crystallogr. C* **2002**, *58*, m129-m132; (b) Ma, K.; Lerner, H.-W.; Scholz, S.; Bats, J. W.; Bolte, M.; Wagner, M. Stepwise assembly and structural characterization of oligonuclear ferrocene aggregates with boron–nitrogen backbone. *J. Organomet. Chem.* **2002**, *664*, 94-105; (c) Nowik, I.; Wagner, M.; Herber, R. H. Bonding, motional anisotropy, and metal atom dynamics of iron in two ferrocene substituted boron ring compounds. *J. Organomet. Chem.* **2003**, *688*, 11-14; (d) Thilagar, P.; Chen, J.; Lalancette, R. A.; Jákľe, F. Reversible Formation of a Planar Chiral Ferrocenylboroxine and Its Supramolecular Structure. *Organometallics* **2011**, *30*, 6734-6741; (e) Tokunana, Y. Boroxine Chemistry: From Fundamental Studies to Applications in Supramolecular and Synthetic Organic Chemistry. *Heterocycles* **2013**, *87*, 31; (f) Appel, A.; Nöth, H. Synthesis and Structures of New Borylferrocenes, and Structures of, 2-Chalcogeno-bis(aminoboryl)[3]ferrocenophanes and 1,1'-Tris(dimethylaminoboryl)[3]ferrocenophane [1, 2]. *Z. Anorg. Allg. Chem.* **2010**, *636*, 2329-2342.
21. Makarov, M. V.; Dyadchenko, V. P.; Antipin, M. Y. Synthesis and structure of tris(4-ferrocenylphenyl)boroxine and its utility in cross-coupling reaction. *Russ. Chem. Bull.* **2004**, *53*, 2768-2773.
22. (a) Ori, A.; Shinkai, S. Electrochemical detection of saccharides by the redox cycle of a chiral ferrocenylboronic acid derivative: a novel method for sugar sensing. *J. Chem. Soc., Chem. Commun.* **1995**, 1771-1772; (b) Lacina, K.; Skládal, P. Ferroceneboronic acid for the electrochemical probing of interactions involving sugars. *Electrochim. Acta* **2011**, *56*, 10246-10252; (c) L. Liu, N. X., J. Du, Q. He, Y. Qin, H. Li, C. Li. A Simple and Rapid Method for Probing of Isomerization of Glucose to Fructose with Ferroceneboronic Acid. *Int. J. Electrochem. Sci.* **2013**, *8*, 9163-9170; (d) Rami Reddy, E.; Trivedi, R.; Giribabu, L.; Sridhar, B.; Pranay kumar, K.; Srinivasa Rao, M.; Sarma, A. V. S. Carbohydrate-Based Ferrocenyl Boronate Esters: Synthesis, Characterization, Crystal Structures, and Antibacterial Activity. *Eur. J. Inorg. Chem.* **2013**, *2013*, 5311-5319.
23. (a) Tlili, A.; Voituriez, A.; Marinetti, A.; Thuery, P.; Cantat, T. Synergistic effects in amphiphilic phosphino-borane catalysts for the hydroboration of CO₂. *Chem. Commun.* **2016**, *52*, 7553-7555; (b) Bresner, C.; Day, J. K.; Coombs, N. D.; Fallis, I. A.; Aldridge, S.; Coles, S. J.; Hursthouse, M. B. Fluoride anion binding by cyclic boronic esters: influence of backbone chelate on receptor integrity. *Dalton Trans.* **2006**, 3660-3667; (c) Aldridge, S.; Fallis, I. A.; Bresner, C.; Day, J. K.; Tatchell, T.; Broomsgrove, A. E. J.; Loveday, M. J., Ferrocenyl boronic acid based sensor for fluoride and cyanide. Patent WO 2008/078092A1: **2008**.
24. (a) Kotz, J. C.; Post, E. W. Ferrocenylboranes. I. Preparation and properties of ferrocenyldichloroborane. *Inorg. Chem.* **1970**, *9*, 1661-1669; (b) Herberhold, M.; Dörfler, U.; Wrackmeyer, B. Dynamic behaviour of some boryl-substituted ferrocenes. *Polyhedron* **1995**, *14*, 2683-2689; (c) Braunschweig, H.; Breitling, F. M.; Kraft, K.; Kraft, M.; Seeler, F.; Stellwag, S.; Radacki, K. Substituted Ferrocenylboranes – Potential Ligand Precursors for ansa-Metallocenes, Constrained Geometry Complexes and ansa-Diamido Complexes. *Z. Anorg. Allg. Chem.* **2006**, *632*, 269-278; (d) Corrente, A. M.; Chivers, T. Syntheses and structures of new alkali-metal boraamidates and ferrocenyl aminoboranes. *New J. Chem.* **2010**, *34*, 1751-1759.
25. Noguchi, H.; Hojo, K.; Suginome, M. Boron-Masking Strategy for the Selective Synthesis of Oligoarenes via Iterative Suzuki–Miyaura Coupling. *J. Am. Chem. Soc.* **2007**, *129*, 758-759.
26. Ihara, H.; Koyanagi, M.; Suginome, M. Anthranilamide: A Simple, Removable ortho-Directing Modifier for Arylboronic Acids Serving also as a Protecting Group in Cross-Coupling Reactions. *Org. Lett.* **2011**, *13*, 2662-2665.
27. Yamamoto, Y.; Takizawa, M.; Yu, X.-Q.; Miyaura, N. Cyclic Triolborates: Air- and Water-Stable Ate Complexes of Organoboronic Acids. *Angew. Chem. Int. Ed.* **2008**, *47*, 928-931.

28. (a) Gillis, E. P.; Burke, M. D. A Simple and Modular Strategy for Small Molecule Synthesis: Iterative Suzuki–Miyaura Coupling of B-Protected Haloboronic Acid Building Blocks. *J. Am. Chem. Soc.* **2007**, *129*, 6716–6717; (b) Li, J.; Grillo, A. S.; Burke, M. D. From Synthesis to Function via Iterative Assembly of N-Methyliminodiacetic Acid Boronate Building Blocks. *Acc. Chem. Res.* **2015**, *48*, 2297–2307.
29. Lennox, A. J. J.; Lloyd-Jones, G. C. Selection of boron reagents for Suzuki–Miyaura coupling. *Chem. Soc. Rev.* **2014**, *43*, 412–443.
30. (a) Bélanger-Chabot, G.; Braunschweig, H.; Roy Dipak, K. Recent Developments in Azaborinine Chemistry. *Eur. J. Inorg. Chem.* **2017**, *2017*, 4353–4368; (b) Davies, G. H. M.; Mukhtar, A.; Saeednia, B.; Sherafat, F.; Kelly, C. B.; Molander, G. A. Azaborinones: Synthesis and Structural Analysis of a Carbonyl-Containing Class of Azaborines. *J. Org. Chem.* **2017**, *82*, 5380–5390; (c) Giustra, Z. X.; Liu, S.-Y. The State of the Art in Azaborine Chemistry: New Synthetic Methods and Applications. *J. Am. Chem. Soc.* **2018**, *140*, 1184–1194.
31. Sanders, R.; Mueller-Westerhoff, U. T. The lithiation of ferrocene and ruthenocene: a retraction and an improvement. *J. Organomet. Chem.* **1996**, *512*, 219–224.
32. Mothana, S.; Grassot, J.-M.; Hall, D. G. Multistep Phase-Switch Synthesis by Using Liquid–Liquid Partitioning of Boronic Acids: Productive Tags with an Expanded Repertoire of Compatible Reactions. *Angew. Chem. Int. Ed.* **2010**, *49*, 2883–2887.
33. Wood, J. L.; Marciasini, L. D.; Vaultier, M.; Pucheault, M. Iron Catalysis and Water: A Synergy for Refunctionalization of Boron. *Synlett* **2014**, *25*, 551–555.
34. Vedejs, E.; Chapman, R. W.; Fields, S. C.; Lin, S.; Schrimpf, M. R. Conversion of Arylboronic Acids into Potassium Aryltrifluoroborates: Convenient Precursors of Arylboron Difluoride Lewis Acids. *J. Org. Chem.* **1995**, *60*, 3020–3027.
35. Lennox, A. J. J.; Lloyd-Jones, G. C. Preparation of Organotrifluoroborate Salts: Precipitation-Driven Equilibrium under Non-Etching Conditions. *Angew. Chem. Int. Ed.* **2012**, *51*, 9385–9388.
36. Mancilla, T.; Contreras, R.; Wrackmeyer, B. New bicyclic organylboronic esters derived from iminodiacetic acids. *J. Organomet. Chem.* **1986**, *307*, 1–6.
37. *Nuclear Magnetic Resonance Spectroscopy of Boron Compounds*, H. Nöth, B. W., P. Diehl, E. F., R. Kosfeld, Ed. Springer-Vorlag: Berlin, **1978**.
38. Nöth, H.; Wrackmeyer, B. Kernresonanzspektroskopische Untersuchungen an Borverbindungen, VII. ^{11}B - und ^{14}N -Kernresonanzstudien an tetrakoordinierten Bor-Stickstoff-Verbindungen. *Chem. Ber.* **1974**, *107*, 3070–3088.
39. (a) Sibi, M. P. Nitrogen-15 NMR spectroscopy: Nitrogen-15 chemical shifts of 1,2-diaminobenzenes and 1,8-diaminonaphthalenes. *Magn. Reson. Chem.* **1991**, *29*, 400–400; (b) Brownlee, R. T. C.; Sadek, M. Natural abundance ^{15}N chemical shifts in substituted benzamides and thiobenzamides. *Magn. Reson. Chem.* **1986**, *24*, 821–826.
40. (a) Nesmeyanov, A. N.; Petrovskii, P. V.; Fedorov, L. A.; Robas, V. I.; Fedin, E. I. The ^{13}C NMR and electronic effects in the pie-cyclopentadienyl derivatives of iron. *Zh. Strukt. Khim.* **1973**, *14*, 8; (b) Braun, S.; Abram, T. S.; Watts, W. E. Carbon-13 NMR spectra of ferrocenes and ferrocenyl-alkylium ions. *J. Organomet. Chem.* **1975**, *97*, 429–441; (c) Koridze, A. A.; Petrovskii, P. V.; Mokhov, A. I.; Lutsenko, A. I. Electronic effects in the cyclopentadienyl ring. The ^{13}C NMR spectra of monosubstituted ferrocenes. *J. Organomet. Chem.* **1977**, *136*, 57–63; (d) Pickett, T. E.; Richards, C. J. Assignment of ^1H NMR chemical shifts in 1,2- and 1,1'-disubstituted ferrocenes. *Tetrahedron Lett.* **1999**, *40*, 5251–5254.
41. Brown, R. A.; Houlton, A.; Roberts, R. M. G.; Silver, J.; Frampton, C. S. Ferrocenyl ligands-III. Bulky ferrocenyl derivatives. 1,1'-Bis(diphenylphosphino)-3,3'-bis(trimethylsilyl)ferrocene. Synthesis, metal complexation and the crystal and molecular structure. *Polyhedron* **1992**, *11*, 2611–2619.
42. Wrackmeyer, B.; Dörfler, U.; Milius, W.; Herberhold, M. Metal-boron interactions in boron-substituted ferrocenes, ruthenocenes and osmocenenes. *Polyhedron* **1995**, *14*, 1425–1431.
43. Scheibitz, M.; Bolte, M.; Bats, J. W.; Lerner, H. W.; Nowik, I.; Herber, R. H.; Krapp, A.; Lein, M.; Holthausen, M. C.; Wagner, M. $\text{C}_5\text{H}_4\text{BR}_2$ Bending in Ferrocenylboranes: A Delocalized Through-Space Interaction Between Iron and Boron. *Chem. Eur. J.* **2005**, *11*, 584–603.
44. Kamiński, R.; Jarzemska, K. N.; Dąbrowski, M.; Durka, K.; Kubsik, M.; Serwatowski, J.; Woźniak, K. Finding Rules Governing Layered Architectures of Trifluoroborate Potassium Salts in the Solid State. *Cryst. Growth Des.* **2016**, *16*, 1687–1700.
45. Dick, G. R.; Woerly, E. M.; Burke, M. D. A General Solution for the 2-Pyridyl Problem. *Angew. Chem. Int. Ed.* **2012**, *51*, 2667–2672.
46. Dick, G. R.; Knapp, D. M.; Gillis, E. P.; Burke, M. D. General Method for Synthesis of 2-Heterocyclic N-Methyliminodiacetic Acid Boronates. *Org. Lett.* **2010**, *12*, 2314–2317.
47. Cheng, C.; Hartwig, J. F. Catalytic Silylation of Unactivated C–H Bonds. *Chem. Rev.* **2015**, *115*, 8946–8975.
48. Ihara, H.; Suginome, M. Easily Attachable and Detachable ortho-Directing Agent for Arylboronic Acids in Ruthenium-Catalyzed Aromatic C–H Silylation. *J. Am. Chem. Soc.* **2009**, *131*, 7502–7503.
49. During the reviewing process, the intramolecular catalytic silylation of ferrocene derivatives was reported by Zhao. Zhao, W.-T.; Lu, Z.-Q.; Zheng, H.; Xue, X.-S.; Zhao, D. Rhodium-Catalyzed 2-Arylphenol-Derived Six-Membered Silacyclization: Straightforward Access toward Dibenzooxasilines and Silicon-Containing Planar Chiral Metallocenes. *ACS Catalysis* **2018**, *8*, 7997–8005.
50. Cheng, C.; Simmons, E. M.; Hartwig, J. F. Iridium-Catalyzed, Diastereoselective Dehydrogenative Silylation of Terminal Alkenes with $(\text{TMSO})_2\text{MeSiH}$. *Angew. Chem. Int. Ed.* **2013**, *52*, 8984–8989.
51. Datta, A.; Kollhofer, A.; Plenio, H. Ir-catalyzed C–H activation in the synthesis of borylated ferrocenes and half sandwich compounds. *Chem. Commun.* **2004**, 1508–1509.
52. Wang, G.; Xu, L.; Li, P. Double N,B-Type Bidentate Boryl Ligands Enabling a Highly Active Iridium Catalyst for C–H Borylation. *J. Am. Chem. Soc.* **2015**, *137*, 8058–8061.
53. Cheng, C.; Hartwig, J. F. Rhodium-Catalyzed Intermolecular C–H Silylation of Arenes with High Steric Regiocontrol. *Science* **2014**, *343*, 853–857.
54. Yamamoto, T.; Ishibashi, A.; Suginome, M. Regioselective Synthesis of o-Benzenediboronic Acids via Ir-Catalyzed o-C–H Borylation Directed by a Pyrazolylaniline-Modified Boronyl Group. *Org. Lett.* **2017**, *19*, 886–889.
55. Mkhali, I. A. I.; Barnard, J. H.; Marder, T. B.; Murphy, J. M.; Hartwig, J. F. C–H Activation for the Construction of C–B Bonds. *Chem. Rev.* **2010**, *110*, 890–931.
56. Ros, A.; Estepa, B.; López-Rodríguez, R.; Álvarez, E.; Fernández, R.; Lassaletta, J. M. Use of Hemilabile N,N Ligands in Nitrogen-Directed Iridium-Catalyzed Borylations of Arenes. *Angew. Chem. Int. Ed.* **2011**, *50*, 11724–11728.
57. Paul, S.; Chotana, G. A.; Holmes, D.; Reichle, R. C.; Maleczka, R. E.; Smith, M. R. Ir-Catalyzed Functionalization of 2-Substituted Indoles at the 7-Position: Nitrogen-Directed Aromatic Borylation. *J. Am. Chem. Soc.* **2006**, *128*, 15552–15553.

